IJC Heart & Vasculature 8 (2015) 122–127

Contents lists available at ScienceDirect

IJC Heart & Vasculature

journal homepage: http://www.journals.elsevier.com/ijc-heart-and-vasculature

Changes in the reference lumen size of target lesions before and after coronary stent implantation: Evaluation with frequency domain optical coherence tomography☆,☆☆

Muneo Kurokawa [a,b], Shiro Uemura [b,c,*], Makoto Watanabe [b], Yoko Dote [b], Yu Sugawara [b], Yutaka Goryo [b], Tomoya Ueda [b], Satoshi Okayama [b], Michinori Kayashima [a], Yoshihiko Saito [b]

[a] Department of Medical Engineering, Nara Medical University, Japan
[b] First Department of Internal Medicine, Nara Medical University, Japan
[c] Cardiovascular Medicine, Kawasaki Medical School, Japan

ARTICLE INFO

Article history:
Received 1 February 2015
Received in revised form 4 May 2015
Accepted 13 June 2015
Available online 17 June 2015

Keywords:
Coronary artery disease
Optical coherence tomography
Percutaneous coronary intervention

ABSTRACT

Objective: In optical coherence tomography (OCT)-guided percutaneous coronary intervention (PCI), stent size is usually determined according to the pre-PCI lumen size of either the distal or proximal reference site. However, the effect of the OCT imaging catheter crossing the target lesion on the reference lumen measurements has not been studied. We evaluated changes in the reference lumen size before and after PCI using frequency domain OCT.
Methods: For 100 consecutive patients with PCI, mean lumen diameter (LD) and lumen area (LA) were measured at the proximal and distal reference sites before and after coronary stent implantation with OCT.
Results: Mean LD and LA of the distal reference site were significantly increased after PCI with stent implantation (2.57 ± 0.6 to 2.62 ± 0.64 mm, $p < 0.01$ and 5.20 ± 2.66 to 5.41 ± 2.54 mm^2, $p < 0.01$, respectively). By contrast, these indices at the proximal reference site were significantly decreased. ROC curve analysis selected MLA of 1.50 mm^2 as the best cutoff value for changes in mean LD. Distal mean LD was markedly increased after PCI in lesions with MLA < 1.50 mm (2.28 ± 0.48 to 2.40 ± 0.17 mm, $P < 0.001$), but did not change in lesions with MLA > 1.50 mm^2. Tissue characteristics were not correlated with changes in reference lumen size.
Conclusions: When we select the stent size during OCT-guided PCI, we need to pay attention to the decrease in the luminal measurement of the reference sites, especially in lesions with tight stenosis.

1. Introduction

Optical coherence tomography (OCT) is a high-resolution intracoronary imaging technology based on near-infrared interferometry. OCT has superior spatial resolution up to 10 to 20 μm, which is approximately 10 times higher than that of conventional intravascular ultrasound (IVUS) imaging [1–3]. In particular, recent clinical studies have shown that new generation frequency domain OCT (FD-OCT) provides more accurate and reproducible quantitative measurements of coronary artery dimensions than IVUS in the clinical setting [4,5]. Furthermore, FD-OCT is superior to IVUS imaging for coronary plaque characterization and detection of suboptimal lesion morphology after coronary stent implantation, such as incomplete stent apposition, intrastent tissue protrusion, or stent edge dissection [6–8]. Based on these advantages in precise visualization of atherosclerotic lesions in coronary arteries, FD-OCT is starting to be used as a guide for percutaneous coronary intervention (PCI) in daily practice.

During OCT-guided PCI, the size of the coronary stent is usually selected according to the pre-PCI mean lumen diameter (LD) of either the distal or proximal reference site. However, it is possible that the reference lumen size changes with hemodynamic alterations within the target coronary artery, such as a pressure drop beyond the baseline region of tight stenosis as well as the presence of the OCT imaging catheter within the target lesion. Therefore, the measurement of reference values with FD-OCT might affect the stent size selected. In fact, previous studies have indicated that the size of the stent selected was significantly smaller with FD-OCT compared to IVUS guidance [9].

The aim of this study was to evaluate changes in the reference lumen size of the target lesion before and after PCI with coronary stent implantation using FD-OCT imaging.

☆ There are no potential conflicts of interest, including related consultancies, shareholdings, and funding grants with regards to this manuscript.
☆☆ All authors take responsibility for all aspects of reliability and freedom from bias for the data presented and their discussed interpretation.

* Corresponding author at: First Department of Internal Medicine, Nara Medical University, 840 Shijo-cho, Kashihara, Nara 634-8522, Japan.
E-mail address: suemura@naramed-u.ac.jp (S. Uemura).

http://dx.doi.org/10.1016/j.ijcha.2015.06.003

2. Methods

2.1. Patients

From January 2013 to March 2014, a consecutive series of 100 patients with single-vessel stable coronary artery disease who underwent FD-OCT-guided PCI with coronary stent implantation were enrolled. Indications for PCI were determined by the results of either pre-procedural myocardial perfusion imaging, exercise electrocardiography, or fractional flow reserve.

Exclusion criteria consisted of the following: (1) ST elevation or non-ST elevation myocardial infarction; (2) lesion with total occlusion; (3) previously stented lesion; (4) angiographically visible thrombus; (5) left main disease; (6) lesion morphology unsuitable for OCT imaging, or (7) unwillingness to participate in this study. This study was approved by the institutional review board of Nara Medical University, and all patients provided written informed consent before cardiac catheterization.

2.2. Diagnostic and therapeutic procedures

Diagnostic coronary angiography was performed in all patients after intracoronary administration of nitroglycerin (0.5 mg). Quantitative coronary angiography (QCA) was performed before and after stent implantation. Briefly, with the use of a guiding catheter for calibration, QCA was performed to measure the reference diameter, minimal lumen diameter with an edge detection system (Medis, Leiden, Netherlands). Lesion length and percent diameter stenosis were then calculated.

All lesions were treated with a single drug-eluting stent implanted through a routine procedure. When selecting the stent edge-landing zone, vessel segments with the following OCT findings were avoided: (1) lipid arc >90°, (2) calcium arc >90°, (3) macrophage infiltration, or (4) thrombus formation.

2.3. FD-OCT image acquisition

FD-OCT images were obtained with the Dragonfly OCT imaging catheter and C7-XR system (C7 system, Dragonfly imaging catheter: LightLab Imaging/St. Jude Medical, Westford, MA). The diameter of the imaging catheter in the optical lens region is 2.7 Fr (0.88 mm). Just before each introduction of the imaging catheter, nitroglycerin (0.5 mg) was repetitively injected via intracoronary. After Z-offset calibration, the OCT imaging catheter was advanced distal to the target lesion over a 0.014-in. conventional angioplasty guide wire through a 6- or 7-Fr guiding catheter. Pullback image acquisition was performed with continuous injection of 2.5 to 3.0 ml/s of X-ray contrast media through the guiding catheter using an injection pump in order to remove blood from the field of view to allow for clear visualization of the vessel wall. The speed of automated pullback was fixed at 36 mm/s. OCT images were acquired at the rate of 5 frames/mm and stored for subsequent analysis.

If OCT visualization of the distal segment beyond the target area of stenosis was inadequate due to under-opacification with contrast medium, the following procedures were attempted to obtain clearer OCT images: (1) antecedent injection of contrast medium into the target coronary artery, (2) immediate advancement of the imaging catheter through the area of tight stenosis during continuous contrast infusion, and (3) starting OCT image acquisition with continuous injection of contrast medium. These steps usually enabled us to obtain clear images beyond the area of tight stenosis.

2.4. OCT data analysis

Quantitative analysis of OCT images was performed with proprietary software offline (C7 system, Dragonfly imaging catheter: LightLab Imaging/St. Jude Medical,).

Using the longitudinal reconstruction OCT views and the lumen profile display software, candidate flames for the minimum lumen area (MLA) of the target lesion were screened. By comparing the lumen areas of 3 consecutive OCT images including the candidate flames, MLA was determined as the smallest lumen area in this series. Mean LD was defined as the mean lumen diameter at the MLA site.

Fig. 1 shows the scheme for measurement of OCT parameters. For the precise comparison of LA and mean LD at reference sites before and after stent implantation, we first determined the distal and proximal reference sites on OCT images obtained after stent implantation. In order to avoid the influence of plaque shift or coronary artery dissection, reference sites 4 mm apart from each edge of the implanted stent

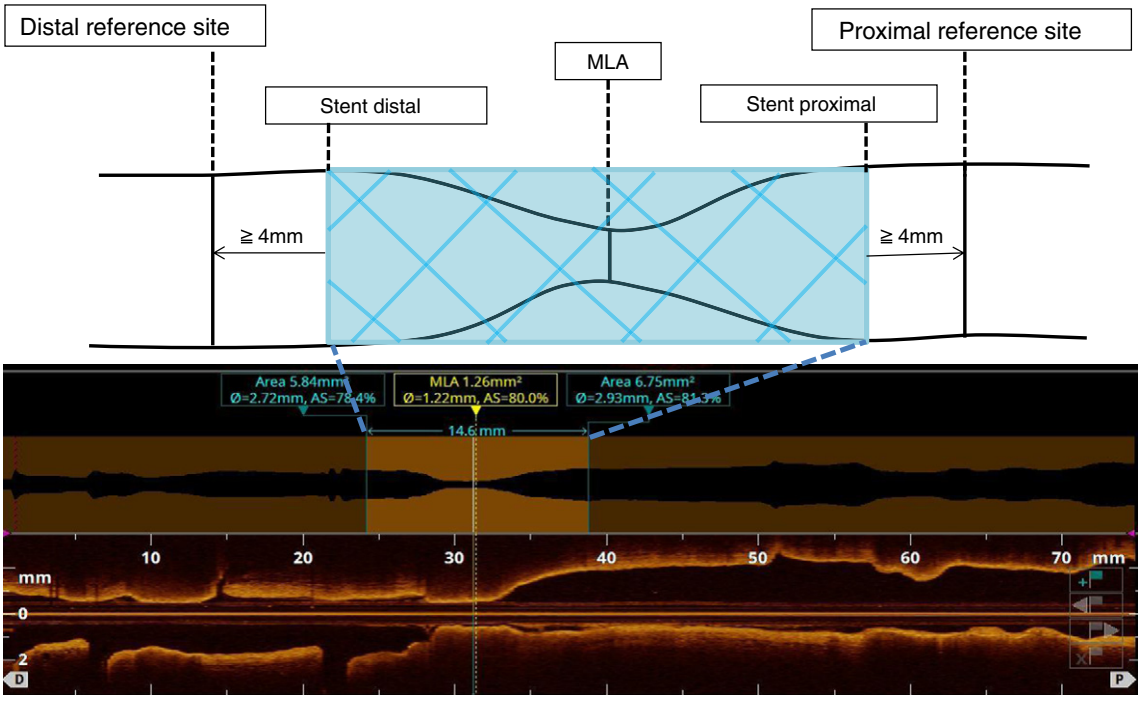

Fig. 1. Schematic methods for OCT measurement of target lesion.

were selected. Pre-interventional OCT reference sites corresponding to the specific coronary region on post-stent OCT images were then extracted. In order to ensure that identical coronary regions were being assessed, corresponding pre- and post-stenting OCT images were identified by the distance from 2 landmarks, such as side branches and stent edges. Reference LA at both the proximal and distal sites was defined as the averaged lumen area of 10 frames (2 mm in length), and mean LD was defined as the mean diameter of the lumen at the MLA site.

Morphological evaluation of OCT images was performed for both proximal and distal reference segments. Discernment of specific tissue types with OCT was accomplished using the definitions of Kume et al. [10]. Based on OCT images at the reference sites, tissue was classified into one of the 4 categories: (1) normal vessel configuration, (2) simple fibrous plaque, (3) intimal layer containing any degree of lipid tissue, or (4) intimal layer containing calcification. Segments with overlapping side branches and poor-quality images were excluded from subsequent analysis.

QCA and quantitative OCT analysis were performed independently by 2 researchers blinded to patient background.

2.5. Statistical analysis

All analyses were performed using JMP statistics version 11 (Cary, NC, USA). All values are expressed as means ± SD for continuous variables, and medians with interquartile ranges (IQRs) or counts and percentages for categorical variables. Continuous variables were compared using the unpaired Student's t-test or Wilcoxon rank-sum test based on the underlying distribution. Categorical data were evaluated using the Pearson chi-square test or 1-way ANOVA, as appropriate. A receiver operating characteristic (ROC) curve was used to determine the best MLS cutoff value for predicting the increment of LA at the distal reference site after PCI. The best cutoff value was defined as the value with the highest Youden's index (sensitivity + specificity − 1). $P < 0.05$ was considered statistically significant.

3. Results

3.1. Patient and lesion characteristics

The clinical background of the study patients is summarized in Table 1. All OCT imaging procedures were complete, and there were no adverse events related to the imaging procedures.

Table 1
Patient characteristics.

	N = 100
Age, years (±SD)	67 ± 12
Male gender	81
Coronary risk factor	
Hypertension	49
Dyslipidemia	64
Diabetes mellitus	39
Current smoker	48
Target imaging vessel	
LAD (left anterior descending coronary artery)	36
LCX (left circumflex coronary artery)	38
RCA (right coronary artery)	26
QCA	
Lesion length, mm	17.2 ± 6.20
MLD, mm	1.20 ± 0.34
Distal reference site, mm	2.63 ± 0.55
Proximal reference site, mm	3.16 ± 0.43
AHA lesion classification	
A	3
B1	41
B2	23
C	33

Sixty-four percent of the lesions were classified as AHA type B lesions. Based on QCA analysis, the mean lesion length was 17.2 ± 6.20 mm and the mean MLA of target lesions was 1.20 ± 0.34 mm according to baseline coronary angiography.

3.2. Quantitative OCT analysis

Table 2 shows the summary of OCT measurements. The mean MLA was 1.27 ± 0.62 mm^2. At the distal reference site, both LA and mean LD were significantly increased after stent implantation (LA: from 5.20 ± 2.66 mm^2 to 5.41 ± 2.54 mm^2, $P = 0.003$; mean LD: from 2.57 ± 0.60 mm to 2.62 ± 0.64 mm, $P < 0.001$). The difference between pre- and post-stent implantation was 0.05 mm. In contrast, both LA and LD at the proximal reference site were significantly decreased after stent implantation (LA: from 7.99 ± 3.95 mm^2 to 7.68 ± 3.90 mm^2, $P < 0.001$; mean LD: from 3.19 ± 0.73 mm to 3.12 ± 0.73 mm, $P < 0.001$).

Fig. 2A shows the ROC curve for MLA at target stenosis in predicting the increase in distal reference site after PCI. The AUC for MLA was 0.78 ($P < 0.001$). When the MLA cut-off value was set at 1.50 mm^2, the sensitivity and specificity were 0.69 and 84%, respectively. Fig. 2B shows a representative case of MLA < 1.5 mm^2. The imaging catheter occupies more than 60% of the cross-sectional lumen area at target lesion.

In lesions with MLA < 1.50 mm^2 ($n = 68$), the distal mean LD was significantly increased (from 2.28 ± 0.48 mm to 2.40 ± 0.17 mm, $P < 0.001$) after stent implantation. The difference was 0.12 mm. On the other hand, no significant changes were observed in the distal mean LD in lesions with MLA > 1.50 mm^2 ($n = 32$, from 2.96 ± 0.68 mm to 2.94 ± 0.65 mm, $P = 0.68$). Proximal mean LD significantly decreased (from 3.00 ± 0.62 mm to 2.94 ± 0.62 mm, $P < 0.001$) after stent implantation. Similar changes were observed in the mean proximal LD and LA in lesions with MLA > 1.50 mm^2 (Table 3, Fig. 3).

3.3. Qualitative OCT analysis

Fig. 4 summarizes the results of the qualitative evaluation of tissue characteristics at reference sites. At the distal reference site, 61% of vessel segments were normal coronary artery, 14% fibrous plaque, 16% lipidic plaque, and 8% calcification. Tissue characteristics at the distal reference site were not correlated with changes in LA and LD at both reference sites. Similar results were observed for the proximal reference site.

4. Discussion

The major findings of this study are: (1) baseline measurements of coronary arterial lumen size at reference sites with FD-OCT are different from post-interventional treatment measurements, (2) pre-interventional reference lumen size significantly changes when MLA of target lesion is smaller than 1.50 mm^2, and (3) these dimensional changes are similar irrespective of tissue characteristics at reference sites.

Table 2
OCT measurements.

	Pre-PCI (n = 100)	Post-PCI (n = 100)	Post–Pre	P value
OCT measurement				
MLA site	LA, mm^2 1.27 ± 0.62			
	LD, mm 1.27 ± 0.27			
Distal reference site				
	LA, mm^2 5.20 ± 2.66	5.41 ± 2.54	0.21 ± 0.74	0.003
	LD, mm 2.57 ± 0.60	2.62 ± 0.64	0.05 ± 0.18	<0.001
Proximal reference site				
	LA, mm^2 7.99 ± 3.95	7.68 ± 3.90	−0.31 ± 0.74	<0.001
	LD, mm 3.19 ± 0.73	3.12 ± 0.73	−0.07 ± 0.13	<0.001

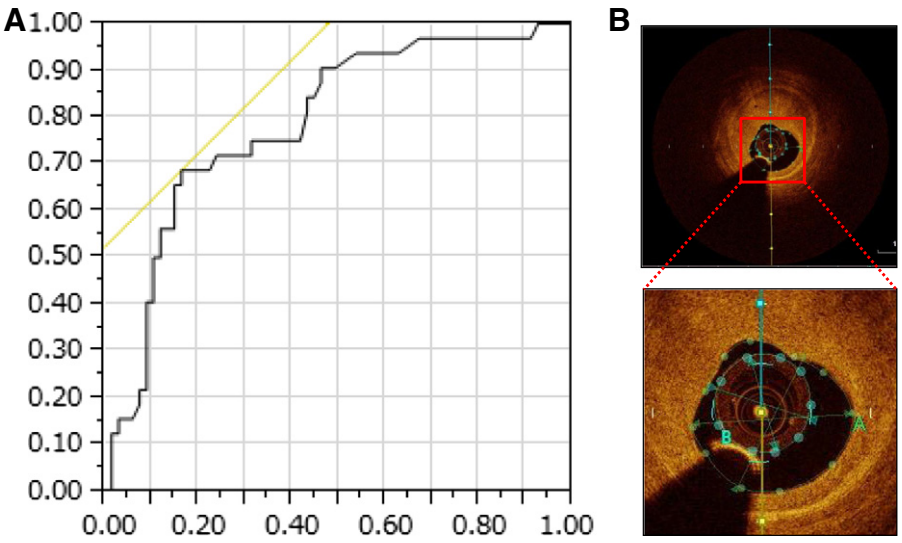

Fig. 2. (A) Receiver operating characteristic curve analysis for MLA at target stenosis in predicting the increase in distal reference site after PCI. The AUC for MLA was 0.78 ($P < 0.001$). When the MLA cut-off value was set at 1.50 mm^2, the sensitivity and specificity were 0.69 and 84%, respectively. (B) A representative case of MLA < 1.5 mm^2. The imaging catheter occupies more than 60% of the cross-sectional lumen area.

4.1. Changes in pre-interventional vessel lumen size

The size of coronary stents is usually selected based on the reference lumen size of target lesions during OCT-guided PCI, and precise lumen measurements are important for selecting the optimal stent size and achieving successful acute results. However, the OCT imaging catheter needs to pass the baseline stenotic lesions in order to measure baseline lumen dimensions at both proximal and distal reference sites in the vessel. Introduction of the imaging catheter intrinsically causes obstructive effects and creates additional artifactual pressure drops beyond the target area of stenosis; these effects possibly result in vessel shrinkage through elastic recoil at the reference sites.

Local pressure-flow characteristics of coronary stenotic lesions have been extensively studied, and it is well established that pressure loss occurs beyond intermediate and severe stenosis even in resting coronary flow conditions as well as at maximal vasodilatation [11,12]. A computer simulation study of trans-lesion hemodynamic changes revealed that the pressure gradient is mainly related to diameter stenosis, not lesion length, and that reductions in the resting trans-lesion pressure occurs when diameter stenosis are more than 60% [13]. Accordingly, the presence of a 2.7-Fr (0.88 mm) imaging catheter could increase the pressure gradient at target lesions with moderate to severe lumen stenosis [13–15].

Table 3
Changes in OCT measurements according to the cut-off MLA value of 1.50 mm^2.

(MLA < 1.50 mm^2, n = 68) (MLA ≥ 1.50 mm^2, n = 32)	Pre PCI	Post PCI	Post–Pre	P value
Distal reference site				
MLA < 1.50 mm^2				
LA, mm^2	4.39 ± 1.79	4.78 ± 1.86	0.39 ± 0.66	<0.001
LD, mm	2.28 ± 0.48	2.40 ± 0.47	0.12 ± 0.17	<0.001
MLA ≥ 1.50 mm^2				
LA, mm^2	7.21 ± 2.97	7.10 ± 2.94	−0.11 ± 0.76	0.41
LD, mm	2.96 ± 0.68	2.94 ± 0.65	−0.02 ± 0.18	0.53
Proximal reference site				
MLA < 1.50 mm^2				
LA, mm^2	7.38 ± 3.04	7.08 ± 3.12	−0.30 ± 0.75	<0.001
LD, mm	3.00 ± 0.62	2.94 ± 0.62	−0.06 ± 0.14	<0.001
MLA ≥ 1.50 mm^2				
LA, mm^2	9.85 ± 4.87	9.53 ± 4.88	−0.32 ± 0.48	<0.001
LD, mm	3.45 ± 0.81	3.39 ± 0.81	−0.06 ± 0.10	<0.001

On the other hand, the relationship between pressure drops and dimensional changes in the lumen of the proximal and distal sites of target lesions has not been well studied in humans. One possible explanation is that the relatively low spatial resolution of quantitative conventional imaging modalities, such as coronary angiography and IVUS, cannot precisely analyze fine changes in coronary vessel dimensions. The present study using FD-OCT demonstrated that OCT observation of target segments is associated with shrinkage of the distal vessel segment beyond the target area of stenosis as well as enlargement of the lumen proximal to the target lesion at baseline before PCI. Furthermore, changes in lumen size were significantly greater when the MLA of the target area of stenosis was less than 1.5 mm^2. In terms of the distal reference site, the net change in mean LD was –0.12 mm, which is almost half of the size variation of most commercially available coronary stents. Accordingly, if we select stent size just equal to OCT-determined distal reference LD, significant strut malapposition could occur at both the distal and proximal stent edges. In terms of the proximal reference site, the pre-intervention mean LD was significantly larger than the post-interventional value, but the net change was small, possibly negligible in clinical setting.

When PCI is guided by conventional time-domain OCT (TD-OCT), additional dimensional changes are anticipated compared to those obtained with FD-OCT. When TD-OCT is used to study coronary arteries, balloon occlusion of coronary arteries is necessary and this procedure decreases coronary perfusion pressure that is not compensated by continuous flush injection; therefore, a higher degree of vessel collapse might occur. Supporting this hypothesis, a previous TD-OCT study showed that the lumen area measurements obtained using a proximal balloon occlusion technique were significantly smaller than those obtained with a non-occlusive technique [16].

In addition, the size of IVUS catheters is similar to that of FD-OCT imaging catheters. Therefore, the degree of coronary pressure depression and vessel collapse at the distal reference site is assumed to be comparable with both imaging modalities. Due to limitations in its spatial resolution, IVUS cannot precisely detect changes in vascular dimensions like FD-OCT imaging.

4.2. Tissue characteristics and changes in vessel lumen size

It has been reported that the local mechanical properties of vascular tissue are different among coronary lesions with various atherosclerotic characteristics. According to studies involving elastography and

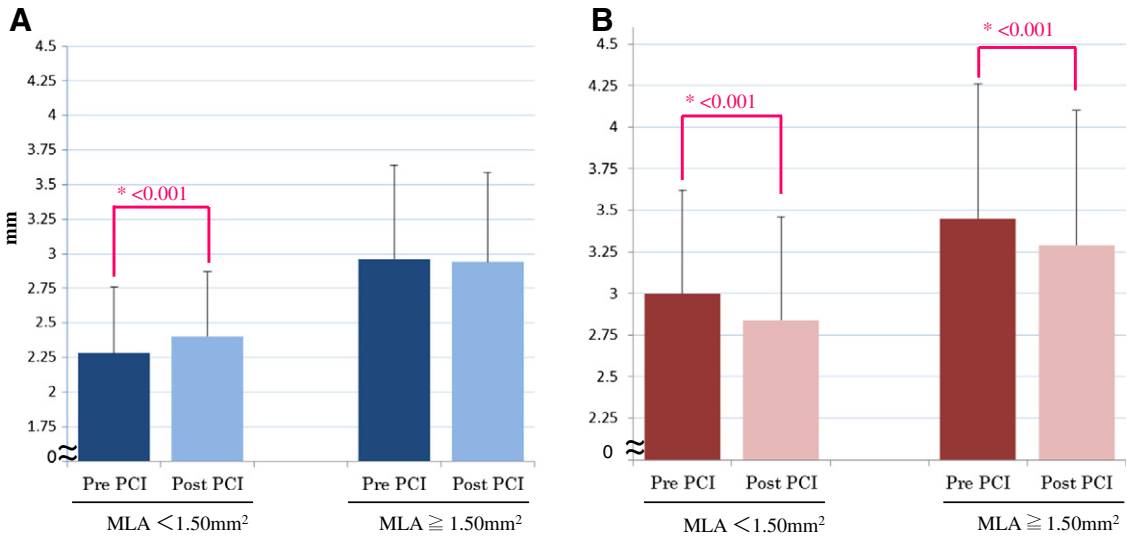

Fig. 3. Changes in the lumen diameter at distal (A) and proximal (B) reference site of target lesion. Each reference is categorized according to 1.50 mm² value of MLA site of target lesion.

palpography of human coronary artery disease [17,18], plaques with lipid accumulation show significantly higher, and plaques with calcium deposition show significantly lower strain values than normal coronary artery segments. From this perspective, the lumen size of coronary segments with lipid accumulation is susceptible to hemodynamic changes. However, in this study, there was no obvious relationship between tissue characteristics at both reference sites and the degree of dimensional changes in lumen diameter after interventional treatment. As described in the Methods section, we intentionally selected the stent edge-landing point to be in a relatively stable vessel segment, and this entry criterion resulted in more than 60% of reference sites classified as having normal or mild fibrous tissue characteristics. It is possible that coronary segments with advanced degrees of atherosclerosis other than the selected reference segments might exhibit larger dimensional changes in lumen size during FD-OCT examination.

4.3. Clinical implications

FD-OCT provides accurate measurements of coronary lumen size with excellent reproducibility even when compared to IVUS. The proper selection of coronary stent size during PCI is essential for successful and optimal revascularization of obstructive target coronary stenosis. Implantation of inappropriately sized stents often results in dissection around the stent edges, under-expansion of stenosis, or malapposition of stent struts to the vascular wall; these peri-procedural compromises are known to be risk factors for development of restenosis and late stent thrombosis in the future [8,19]. Based on our results, the PCI operator always needs to be aware of dimensional changes of the reference sites, especially in cases with tight stenosis when the decision of stent implantation is guided by intravascular imaging modalities. A recent study by Habara et al [9] showed that the minimum stent area was smaller in FD-OCT-guided PCI compared with IVUS-guided PCI. One

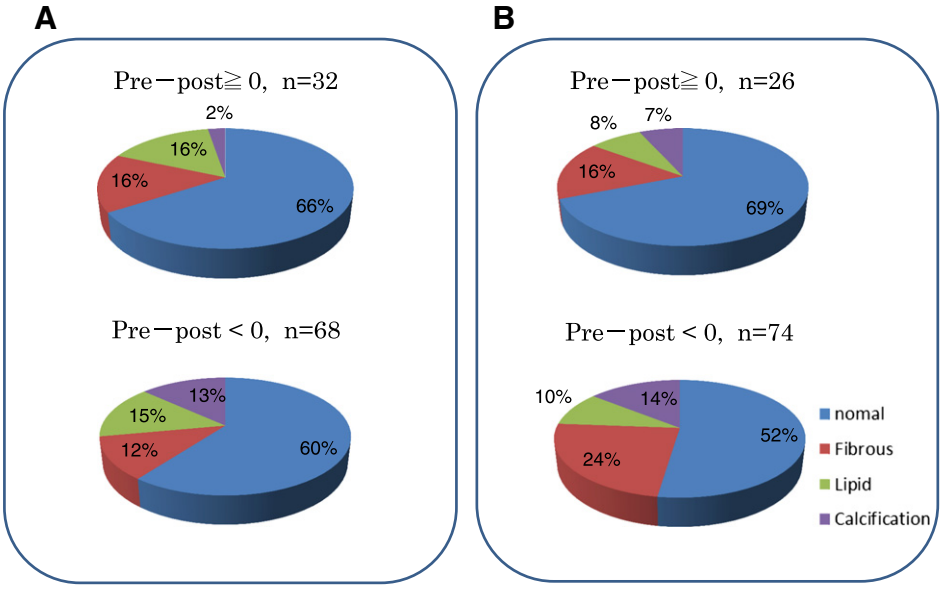

Fig. 4. OCT tissue characteristics at distal (A) and proximal (B) reference site of target lesion. There were no differences in the distribution of tissue characteristics according to the changes in lumen diameter of pre- and post-PCI.

reason for this observation might be due to the selection of stent size according to baseline distal reference diameters with OCT guidance. Future development of imaging catheters with smaller profiles might minimize such alterations in vessel size during intravascular image acquisition.

In addition, OCT imaging is very sensitive to detect suboptimal lesion morphologies after stent implantation in the comparison with IVUS [8]. Although long-term importance of these acute complication during stent implantation have not been established, OCT helps us to optimize the final results for interventional procedure.

4.4. Study limitations

There are several limitations in this study. First, FD-OCT requires the guide wire to be kept in the vessel during image acquisition. The shadow from the guide wire can affect measurements of the lumen area. Second, the injection rate for the contrast media was chosen by each individual operator during FD-OCT image acquisition. Higher injection rates and volumes increase shear stress, which could have affected the measured values. Third, OCT sometimes fails to measure vessel area of coronary arteries, one of the important parameter of stent sizing, because of relatively shallow penetration depth of light into vascular tissue, especially at vessel segment with lipid accumulation and positive remodeling. However, most of the tissue characteristics at reference segments are free from large lipid pool or positive remodeling, at where we perform measurement for selecting stent size of implantation. Finally, systemic blood pressure varies among the patient population, so pressure differences across target areas of stenosis might be different even with similar degrees of diametric stenosis.

5. Conclusions

This study demonstrated that placement of an OCT imaging catheter across an area of significant coronary artery stenosis results in decreased luminal area at the distal reference site. When we select the stent size during OCT-guided PCI, we need to pay attention to the decrease in the luminal measurement of the reference sites, especially in lesions with tight stenosis.

References

[1] M.E. Brezinski, G.J. Tearney, B.E. Bouma, J.A. Izatt, M.R. Hee, E.A. Swanson, et al., Optical coherence tomography for optical biopsy, Prop. Demonstration Vasc. Pathol. Circ. 93 (6) (1996) 1206–1213.
[2] I.K. Jang, B.E. Bouma, D.H. Kang, S.J. Park, S.W. Park, K.B. Seung, et al., Visualization of coronary atherosclerotic plaques in patients using optical coherence tomography: comparison with intravascular ultrasound, J. Am. Coll. Cardiol. 39 (4) (2002) 604–609.
[3] G.J. Tearney, E. Regar, T. Akasaka, T. Adriaenssens, P. Barlis, H.G. Bezerra, et al., Consensus standards for acquisition, measurement, and reporting of intravascular optical coherence tomography studies: a report from the International Working Group for Intravascular Optical Coherence Tomography Standardization and Validation, J. Am. Coll. Cardiol. 59 (12) (2012) 1058–1072.
[4] T. Kubo, T. Akasaka, J. Shite, T. Suzuki, S. Uemura, B. Yu, et al., OCT compared with IVUS in a coronary lesion assessment: the OPUS-CLASS study, JACC Cardiovasc Imaging 6 (10) (2013) 1095–1104.
[5] S. Tahara, H.G. Bezerra, M. Baibars, H. Kyono, W. Wang, S. Pokras, et al., In vitro validation of new Fourier-domain optical coherence tomography, EuroIntervention : J. EuroPCR Collab. Work. Group Interv. Cardiol. Eur. Soc. Cardiol. 6 (7) (2011) 875–882.
[6] S. Uemura, Invasive imaging of vulnerable atherosclerotic plaques in coronary artery disease, Circ. J. Off. J. Japan. Circ. Soc. 77 (4) (2013) 869–875.
[7] F. Prati, L. Di Vito, G. Biondi-Zoccai, M. Occhipinti, A. La Manna, C. Tamburino, et al., Angiography alone versus angiography plus optical coherence tomography to guide decision-making during percutaneous coronary intervention: the Centro per la Lotta contro l'Infarto-Optimisation of Percutaneous Coronary Intervention (CLI-OPCI) study, EuroIntervention : J. EuroPCR Collab. Work. Group Interv. Cardiol. Eur. Soc. Cardiol. 8 (7) (2012) 823–829.
[8] T. Kubo, A. Tanaka, H. Kitabata, Y. Ino, T. Tanimoto, T. Akasaka, Application of optical coherence tomography in percutaneous coronary intervention, Circ. J. Off. J. Japan. Circ. Soc. 76 (9) (2012) 2076–2083.
[9] M. Habara, K. Nasu, M. Terashima, H. Kaneda, D. Yokota, E. Ko, et al., Impact of frequency-domain optical coherence tomography guidance for optimal coronary stent implantation in comparison with intravascular ultrasound guidance, Circ Cardiovasc Interv. 5 (2) (2012) 193–201.
[10] T. Kume, T. Akasaka, T. Kawamoto, N. Watanabe, E. Toyota, Y. Neishi, et al., Assessment of coronary arterial plaque by optical coherence tomography, Am. J. Cardiol. 97 (8) (2006) 1172–1175.
[11] K.L. Gould, Pressure-flow characteristics of coronary stenoses in unsedated dogs at rest and during coronary vasodilation, Circ. Res. 43 (2) (1978) 242–253.
[12] H.V. Anderson, G.S. Roubin, P.P. Leimgruber, W.R. Cox, J.S. Douglas Jr., S.B. King III, et al., Measurement of transstenotic pressure gradient during percutaneous transluminal coronary angioplasty, Circulation 73 (6) (1986) 1223–1230.
[13] R.K. Banerjee, L.H. Back, M.R. Back, Y.I. Cho, Physiological flow simulation in residual human stenoses after coronary angioplasty, J. Biomech. Eng. 122 (4) (2000) 310–320.
[14] R.K. Banerjee, L.H. Back, M.R. Back, Y.I. Cho, Catheter obstruction effect on pulsatile flow rate–pressure drop during coronary angioplasty, J. Biomech. Eng. 121 (3) (1999) 281–289.
[15] R.K. Banerjee, L.H. Back, M.R. Back, Effects of diagnostic guidewire catheter presence on translesional hemodynamic measurements across significant coronary artery stenoses, Biorheology 40 (6) (2003) 613–635.
[16] N. Gonzalo, P.W. Serruys, H.M. Garcia-Garcia, G. van Soest, T. Okamura, J. Ligthart, et al., Quantitative ex vivo and in vivo comparison of lumen dimensions measured by optical coherence tomography and intravascular ultrasound in human coronary arteries, Rev. Esp. Cardiol. 62 (6) (2009) 615–624.
[17] J.A. Schaar, A.F. van der Steen, F. Mastik, R.A. Baldewsing, P.W. Serruys, Intravascular palpography for vulnerable plaque assessment, J. Am. Coll. Cardiol. 47 (8 Suppl.) (2006) C86–C91.
[18] G.A. Rodriguez-Granillo, H.M. Garcia-Garcia, M. Valgimigli, J.A. Schaar, R. Pawar, W.J. van der Giessen, et al., In vivo relationship between compositional and mechanical imaging of coronary arteries. Insights from intravascular ultrasound radiofrequency data analysis, Am. Heart J. 151 (5) (2006) e1–e6 1025.
[19] G.F. Attizzani, D. Capodanno, Y. Ohno, C. Tamburino, Mechanisms, pathophysiology, and clinical aspects of incomplete stent apposition, J. Am. Coll. Cardiol. 63 (14) (2014) 1355–1367.